Revealing an Interconnected Interfacial Layer in Solid-State Polymer Sodium Batteries

Zhao, Chenglong; Liu, Lilu; Lu, Yaxiang; Wagemaker, Marnix; Chen, Liquan; Hu, Yong Sheng

DOI
10.1002/anie.201909877

Publication date
2019

Document Version
Accepted author manuscript

Published in
Angewandte Chemie - International Edition

RESEARCH ARTICLE

Revealing an Interconnected Interfacial Layer in Solid-State Polymer Sodium Batteries

Chenglong Zhao, Lilu Liu, Yaxiang Lu*, Marnix Wagemaker*, Liquan Chen, and Yong-Sheng Hu*

Abstract: Rechargeable sodium batteries are receiving increasing attention as potential technology for large-scale energy storage systems owing to the abundant nature and low cost of Na. Replacing the commonly used nonaqueous liquid electrolytes with polymer solid electrolytes, is expected to provide new opportunities to develop safer batteries with higher energy densities. However, this poses scientific challenges, specifically related to the interface between the Na-metal anode and polymer electrolytes, the properties and failure mechanisms of which remain elusive. Driven by systematically investigating the interface properties, an improved interface is established *in-situ*, between a composite Na/C metal anode and electrolyte. The observed chemical bonding between carbon matrix of anode with solid polymer electrolyte, prevents delamination, and leads to more homogeneous plating and stripping, which reduces/suppresses dendrite formation. Full solid-state polymer Na-metal batteries, using a high mass loaded $Na_3V_2(PO_4)_3$ cathode, exhibit ultrahigh capacity retention of >92% after 2,000 cycles and >80% after 5,000 cycles, as well as the outstanding rate capability. As such, the new approach and demonstrated cycling stability, present a promising route towards realizing stable solid-state polymer Na-metal batteries.

Introduction

Sodium-based batteries have been regarded as promising candidates for smart grid-scale energy storage because of the abundance of Na sources and low cost.[1] To meet the requirement of batteries with higher energy densities, introducing Na metal anodes is generally recognized as an ideal choice owing to its theoretical capacity (~1166 mAh g^{-1}) and low electrochemical potential (-2.71 V *vs.* standard hydrogen electrode, SHE).[2] However, several challenges need to be overcome, including high reactivity with organic liquid electrolytes and unstable Na^+ plating/stripping process, which leads to capacity fading during long-term cycling and safety concerns.[2a, 3]

Solid electrolytes are gaining increasing attention, being less flammable and the potential ability to reduce/suppress the growth of Na-dendrites.[4] However, inorganic ceramic solid electrolytes provide poor interface connectivity with the electrodes due to volumetric changes and uneven Na^+ plating/stripping during cycling. This results in an increase of interfacial resistance, which lowers the reversible capacity and cycling stability. Solid polymer electrolytes (SPE) have the advantages of high-volume utilization, good film-forming ability, light weight and simple/scalable preparation processes, and have been widely investigated during the past several years.[5] Moreno *et al.*, reported a SPE where $Na[(CF_3SO_2)_2N]$ (NaTFSI) and poly(ethylene oxide) (PEO) were blended to achieve an ionic conductivity of ~1.1×10^{-3} S cm^{-1} at 80 °C.[5b] Ma *et al.*, reported a Na[(FSO_2)(n-$C_4F_9SO_2$)N]-based polymer electrolyte, the application of which in solid-state Na||SPE||$NaCu_{1/9}Ni_{2/9}Fe_{1/3}Mn_{1/3}O_2$ cells showed capacity retention of ~70% after 150 cycles at 80 °C.[5a] Compared to inorganic ceramic electrolytes, organic SPEs are generally more ductile and provide opportunities to bond with electrodes, resulting in a smaller interfacial resistance. Therefore, polymer interfacial layers or composite polymer/ceramic electrolytes are frequently used to improve the interface connectivity.[6] Zhou *et al.*, reported a sandwich configuration of a polymer/ceramic-pellet/polymer electrolyte in an solid-state Na-metal battery. Enhanced cycling was suggested to be the result of adding a polymer electrolyte layer, which improved the interface wettability between Na-metal anode and solid ceramic electrolyte.[6b]

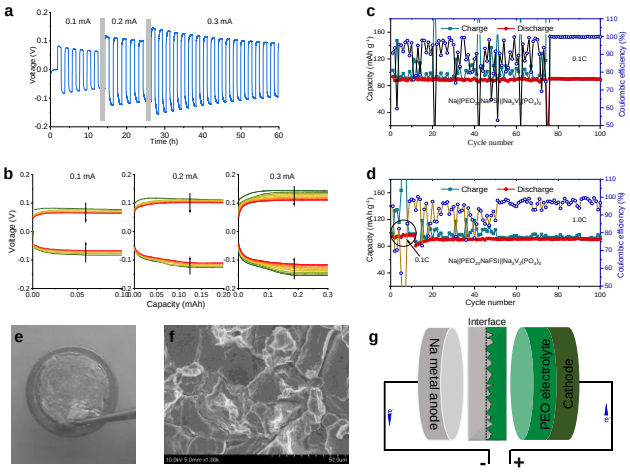

Figure 1. Electrochemical performance of PEO_{20}NaFSI polymer electrolytes in Na||PEO_{20}NaFSI||Na symmetric cells and in Na||PEO_{20}NaFSI||$Na_3V_2(PO_4)_3$ full cells. (a) Voltage curves of the symmetric Na||PEO_{20}NaFSI||Na cells at current densities of 0.1, 0.2 and 0.3 mA at 80 °C. The diameter of Na-metal anodes is 10 mm and the corresponding area is 0.785 cm^2. (b) Capacity curves of the symmetric cells. Charge-discharge capacity and Coulombic efficiency (CE) of Na||PEO_{20}NaFSI||$Na_3V_2(PO_4)_3$ full cells at the rate of (c) 0.1C and (d) 1.0C

[a] C. Zhao, L. Liu, Dr. Y. Lu, Prof. L. Chen, Prof. Y.-S. Hu
Key Laboratory for Renewable Energy, Beijing Key Laboratory for New Energy Materials and Devices, Beijing National Laboratory for Condensed Matter Physics, Institute of Physics, Chinese Academy of Sciences, Beijing 100190 (China)
E-mail: yxlu@aphy.iphy.ac.cn, yshu@aphy.iphy.ac.cn
[b] C. Zhao, L. Liu, Dr. Y. Lu, Prof. Y.-S. Hu
Center of Materials Science and Optoelectronics Engineering, University of Chinese Academy of Sciences, Beijing 100049 (China)
[c] Prof. M. Wagemaker
Department of Radiation Science and Technology, Delft University of Technology, Mekelweg 15, 2629JB Delft, (the Netherlands)
E-mail: m.wagemaker@tudelft.nl
[d] Prof. Y.-S. Hu
Yangtze River Delta Physics Research Center Co. Ltd, Liyang 213300 (China)
Supporting information for this article is given via a link at the end of the document.

(~117 mA g^{-1}), respectively. (e) Digital photo image and (f) scanning electron microscope (SEM) image of Na-metal anode after 100 cycles in the full cells. (g) Schematic illustration of the interfacial phase for solid-state polymer Na-metal batteries.

Although the above indicates that SPEs offer the possibility to maintain good interfacial contact with Na-metal anodes, long-term revesible cycling is very challenging and little is known about the nature of the SPE-Na-metal interface and how it can be further improved. By investigating the interface chemistry between the Na-metal anode and polymer electrolytes, this work provides in depth understanding, based on which a rational strategy is demonstrated to realize highly stable solid-state polymer Na-metal batteries. The electrochemical performance of a typical polymer electrolyte, PEO plasticized by sodium bis(fluorosulfonyl) imide (NaFSI) with a molar ratio of EO/Na^+ = 20 (PEO_{20}NaFSI), paired with the commonly used pure Na-metal-foil anode is shown in Figure 1. Figure 1 (a) and (b) display galvanostatic cycling at 80 °C in symmetric Na||PEO_{20}NaFSI||Na cells at different current densities. A large polarization during Na^+ plating/stripping is observed for several initial cycles, as well as an increase in polarization during subsequent cycles at higher current densities. Similar observations were also found in symmetric Na||PEO_{20}NaFSI||Na[5c], Na||PEO_{20}-$NaClO_4$-SiO_2||Na[7] and Li||PEO-LiTFSI||Li[8] cells. In addition, Na||PEO_{20}NaFSI||$Na_3V_2(PO_4)_3$ full cells exhibit unstable cycling during the initial cycles in Figure 1 (c), resulting in a strongly fluctuating Coulombic efficiency (CE). When the current density is increased from 0.1 to 1.0 C, the number of initial cycles that displays a large fluctuation in the CE is reduced to some extent as shown in Figure 1 (c) and (d), possibly related to the presence of more Na-metal nucleation sites induced by the higher current densities.[9] The origin of the fluctuating CE appears to be unstable discharging, suggesting contact loss of the Na-metal anode during stripping. This implies that the interface connectivity between the SPE and the Na-metal-foil anode is poor before during the initial cycling.

In this work, 10 *wt.*% PEO is added to the cathode mixture, which has been demonstrated as an effective method to improve the interface connectivity between SPE and cathode.[5a, 5c, 6a, 8a] The digital photo and scanning electron microscope (SEM) images of the Na-metal-foil anode from full cells after 100 cycles at 0.1C are shown in Figure 1 (e) and (f). Compared to the blended structure of the cathode side between $Na_3V_2(PO_4)_3$ and the PEO_{20}NaFSI electrolyte, the Na-metal anode can be easily separated from the electrolyte, and a fractured surface is observed. The above further confirms a poor interfacial contact between the SPE and the pure Na-metal-foil anode. Moreover, the contact points between the PEO electrolyte and the Na-metal anode will be lost on repeated Na^+-stripping from the host matrix during long-term cycling, resulting in the rough morphology shown in Figure 1 (f) and illustrated in Figure 1 (g).

Results and Discussion

To improve the interface connectivity between the Na-metal anode and the polymer electrolytes, an initial consideration is that the SPE organic polymer host mainly consists of C and O atomic species having an electronegativity of 2.55 and 3.44, respectively. These result in ionic bonds with Li and Na which are less strong and flexible as covalent bonds for instance. One option may be blending PEO with metallic Na, however, this is very challenging because of the high reactivity of metallic Na. A more promising host matrix for Na-metal is carbon, which is stable towards metallic Na even at temperatures exceeding >300 °C.[11] Moreover, it offers the possibility to establish strong covalent bonds (*e.g.,* C-C, C-O, C=O) owing to reaction between the carbon matrix and the polymer electrolyte. Thus, by introducing carbon in the Na-metal anode, a matrix is introduced that can bond with the PEO species of the SPE, which aims to prevent delamination. Additionally, the ionic and electronic conductivities of the carbon matrix can be expected to promote Na^+ stripping and plating. Composite Na/C metal anodes have been reported widely,[11] showing enhanced performance in organic liquid electrolytes. At present, we aim to use this strategy to improve the interface connectivity between the SPE and the Na-metal anodes, and investigate in detail the PEO_{20}NaFSI polymer electrolyte in combination with a composite Na/C metal anode.

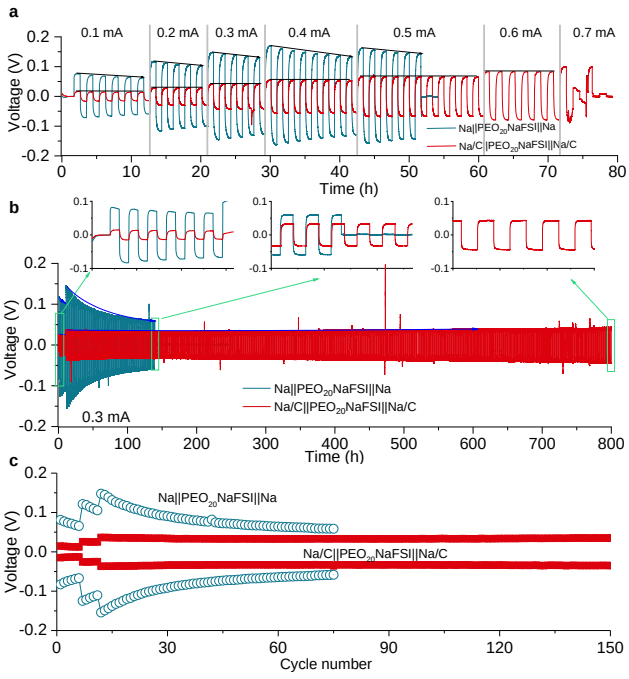

Figure 2. Galvanostatic cycling of symmetric Na||PEO_{20}NaFSI||Na and Na/C||PEO_{20}NaFSI||Na/C cells at 80 °C. (a) Rate performance from 0.1 to 0.7 mA. Comparison of the (b) long-term cycling stability of symmetric cells and (c) voltage curves of the first five cycles at a current density of 0.1 mA, the second five cycles at a current density of 0.2 mA, and subsequent cycles at 0.3 mA.

Figure S1 (a) shows SEM and optical images of the as-prepared PEO/NaFSI polymer electrolyte with a molar ratio of EO/Na^+=20. The thickness of this self-supporting membrane is around 200 µm. The surface is relatively homogeneous with a

random distribution of pores (Supporting information, Figure S2). The structural properties, electrochemical stability, thermal stability, and phase transition behaviour of the as-prepared $PEO_{20}NaFSI$ polymer electrolyte are presented in Figure S3-5. These results are consistent with what was reported previously.[13] The temperature-dependent ionic conductivity of the $PEO_{20}NaFSI$ polymer electrolyte is exhibited in Figure S1 (b), where the ionic conductivity is about 10^{-7} S cm^{-1} at 30 ^{o}C. The conductivity rapidly increases on raising the temperature to ~60 ^{o}C, after which the conductivity increases less rapidly with temperature, corresponding to the glass temperature of crystalline PEO at ~65 ^{o}C as shown in Figure S6. The ionic conductivity reaches ~10^{-4} S cm^{-1} between 60 to 80 ^{o}C, enabling the operation of a solid-state Na battery. The composite Na/C metal anode was prepared by impregnating molten Na into commercially available carbon cloth at 300 ^{o}C (Figure S7).[12] After the infusion of molten Na, the thickness of the composite Na/C metal anode is about 250 µm as shown in Figure S1 (c), and the pores between the carbon fibres appear to be filled completely by molten Na in Figure S1 (d). The additional advantage of the three-dimensional carbon host bonding with the SPE, is that it will distribute the oxidation/reduction over a larger surface area, hence lowering the local current density in the composite Na/C anode. Both the carbon matrix functionality and the distribution of the plating/stripping activity can thus be expected to improve the reversible cycling.

The voltage profiles of symmetric Na||$PEO_{20}NaFSI$||Na and Na/C||$PEO_{20}NaFSI$||Na/C cells are shown in Figure 2. The cells are first cycled at different current densities from 0.1 to 0.7 mA at 80 °C, the results of which are shown in Figure 2 (a). As mentioned already, a large polarization is commonly observed during the initial cycles for symmetric Na||$PEO_{20}NaFSI$||Na cells, and an increased current density appears to lower the overpotentials during subsequent cycles. In contrast, the symmetric Na/C||$PEO_{20}NaFSI$||Na/C cell shows smooth voltage profiles during cycling with much lower overpotentials. When the current density is increased to 0.5 mA, the Na||$PEO_{20}NaFSI$||Na symmetric cell fails after a few cycles, however, the Na/C||$PEO_{20}NaFSI$||Na/C cell cycles reversibly even at 0.6 mA with a very low overpotential of ±80 mV. The stable voltage curves, as shown in Figure S8, suggest that a stable interface connection is established during the heat treatment of the cells. Apparently, the activation process observed for pure Na-metal anodes is not present in the Na/C||$PEO_{20}NaFSI$||Na/C cells. The result is that the symmetric Na/C||$PEO_{20}NaFSI$||Na/C cells can be cycled continuously over 800 h at 0.3 mA, displaying stable voltage curves, as demonstrated in Figure 2 (b). For comparison, the voltage of the Na||$PEO_{20}NaFSI$||Na cells drops to zero after 138 h, see Figure 2 (b) and (c), signifying battery failure through a short circuit. This further suggests that the interface between the PEO polymer matrix and the Na-metal-foil anode is unstable, and decays during the long-term cycling. The cycling stability of the symmetric Na/C||$PEO_{20}NaFSI$||Na/C cells is also evaluated at a higher current density of 0.5 mA, shown in Figure S9 and S9, demonstrating stable cycling over 650 h with an average overpotential around ±75 mV.

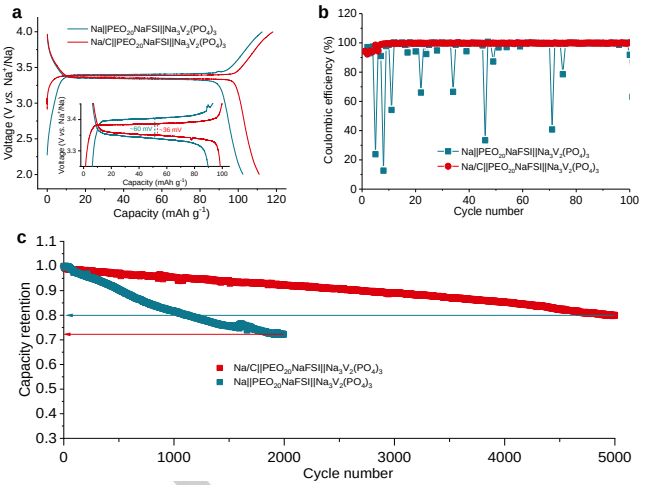

Figure 3. Electrochemical performance of $PEO_{20}NaFSI$ polymer electrolytes in full cells. (a) Charge-discharge curves at a scan rate of 0.1C in the voltage range of 2.0-4.0 V where the inset compares the overpotentials. (b) CE of Na||$PEO_{20}NaFSI$||$Na_3V_2(PO_4)_3$ and Na/C||$PEO_{20}NaFSI$||$Na_3V_2(PO_4)_3$ full cells at a rate of 2.0C and 4.0C, respectively, with the first three cycles at 0.1C in the voltage range of 2.0-4.0 V. (c) Capacity retention of Na||$PEO_{20}NaFSI$||$Na_3V_2(PO_4)_3$ and Na/C||$PEO_{20}NaFSI$||$Na_3V_2(PO_4)_3$ full cells.

To study the performance of the pure Na metal and the composite Na/C metal anodes in full-cell solid-state polymer Na-metal batteries, the Na anodes were tested in combination with $Na_3V_2(PO_4)_3$ as the cathode. The rate capability and long-term cycling stability were evaluated for a relatively large mass loading of 6-8 mg cm^{-2}. Detailed information on the cathode structure and morphology is presented in Figure S11 and S12, Table S1 and S2. The charge-discharge curves at a rate of 0.1C in the voltage range of 2.0-4.0 V are shown in Figure 3 (a). The Na/C||$PEO_{20}NaFSI$||$Na_3V_2(PO_4)_3$ full cells exhibit a larger reversible capacity, ~111 mAh g^{-1}, and a smaller overpotential of ~36 mA, as compared to the ~102 mAh g^{-1} and ~60 mA for the Na||$PEO_{20}NaFSI$||$Na_3V_2(PO_4)_3$ cells. The composite Na/C metal anode also demonstrates a much better rate performance, as shown in Figure S23 and Table S3, for instance amounting 77.9 mAh g^{-1} at 8C compared to 5.2 mAh g^{-1} for a pure Na metal anode. The error bar of the capacity is ±0.1 mAh g^{-1}. The rate and cycling performance of Na/C||$PEO_{20}NaFSI$||$Na_3V_2(PO_4)_3$ full cells is further tested at increased current densities, as shown in Figure S24, where a reversible capacity of about ~92 mAh g^{-1} is achieved at 2.0C during 300 cycles. The long-term cycling stability of the full cells, cycled at 2.0C for Na||$PEO_{20}NaFSI$||$Na_3V_2(PO_4)_3$ and at 4.0C for Na/C||$PEO_{20}NaFSI$||$Na_3V_2(PO_4)_3$, demonstrates a discharge capacity of 86.0 mAh g^{-1} for both anodes. As shown in Figure 3 (b), Figure S25 and S15, the CE of Na||$PEO_{20}NaFSI$||$Na_3V_2(PO_4)_3$ cell experiences drastic fluctuations during the initial cycles, which stabilizes during subsequent cycles. Nevertheless, the capacity decays towards 72% after 2,000 cycles. In contrast, the composite Na/C metal anode reaches a capacity retention above 92% at 2,000 cycles, as shown in Figure 3 (c). Superior cycling stability of the composite Na/C metal anode is further demonstrated in Figure S27 and S17 by a high capacity retention of >80% after 5,000 cycles, >70% after 8,000 cycles. The results demonstrate that the

composite Na/C metal anode enables high-stable solid-state polymer Na-metal batteries.

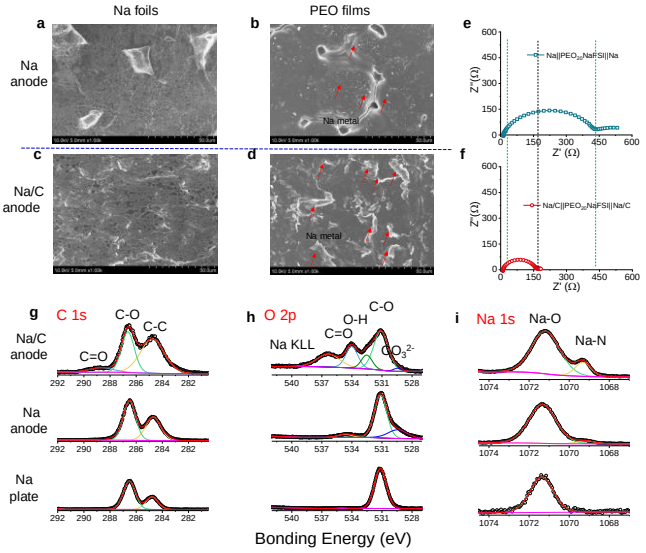

Figure 4. Interface properties of the pristine symmetric cells. SEM images of Na foils and PEO films in (a) and (b) of Na||PEO_{20}NaFSI||Na cells, (c) and (d) of Na/C||PEO_{20}NaFSI||Na/C cells. The assembled symmetric cells were heated to 80 °C for 2 h to establish contact between polymer electrolytes and electrodes prior to the measurements. Electrochemical impedance spectroscopy (EIS) measurements of (e) Na||PEO_{20}NaFSI||Na and (f) Na/C||PEO_{20}NaFSI||Na/C cells. X-ray photoelectron spectra (XPS) of (g) C 1s, (h) O 2p and (i) Na 1s for the composite Na/C anode, Na-metal anode and the pure Na plate.

To investigate the role of the carbon matrix in the Na/C anodes the interface properties between SPE and both pure Na-metal and Na/C anodes are investigated before and after cycling of the cells. Similar to previous studies on solid-state polymer batteries, a pre-heating process is used to enhance the contact between electrolytes and electrodes before the operation of cells.[5c, 7-8] In this work, the symmetric Na|PEO_{20}NaFSI|Na and Na||PEO_{20}NaFSI||$Na_3V_2(PO_4)_3$ cells are also heated to 80 °C for 2 h before operation. Figure 4 (a)-(d) shows the difference in morphology after the preheating for both the Na anodes and PEO membranes, after separating these from each other. Compared to the pure Na foils, shown in Figure S29, the disassembled Na foil in Figure 4 (a) displays obvious delaminated regions, in combination with a fractured morphology, indicating a poor interfacial connection as shown in Figure S20. In contrast, the Na/C anode, removed from the prepared Na/C||PEO_{20}NaFSI||Na/C cell, exhibits signs of tearing and more traces of residual metallic Na on the corresponding PEO films, comparing Figure 4 (d) and Figure 4 (b). After pre-heating for 2h, Na/C||PEO_{20}NaFSI||Na/C cell has a total resistance of ~175 Ω, obtained from electrochemical impedance spectroscopy (EIS), which is about 2.5 times smaller than that of Na||PEO_{20}NaFSI||$Na_3V_2(PO_4)_3$. To gain understanding of the improved interface connectivity of the composite Na/C anodes, interface components of the two Na-metal anodes are analysed by X-ray photoelectron spectra (XPS) as shown in 5 (g)-(i) and Figure S21. The observed peaks around 289 eV in the C 1s spectrum and around 534 eV in the O 2p spectrum reveal the formation of "C=O" bonds[13] on the surface of composite Na/C anode after the pre-heating treatment, which are not presented at the pure Na-metal anodes. Additionally, a stronger component at around 1069.5±0.1 eV in the Na 1s spectrum is observed for the composite Na/C anode as compared to the pure Na-metal anode, where the Na-N species are expected to be a result of the reaction between the NaFSI salt and the Na/C anode. These results indicate that the interface contact of the composite Na/C with the SPE is due to chemical bonding of the SPE with the carbon matrix of the anode, which is established during the preheating treatment before battery cycling.

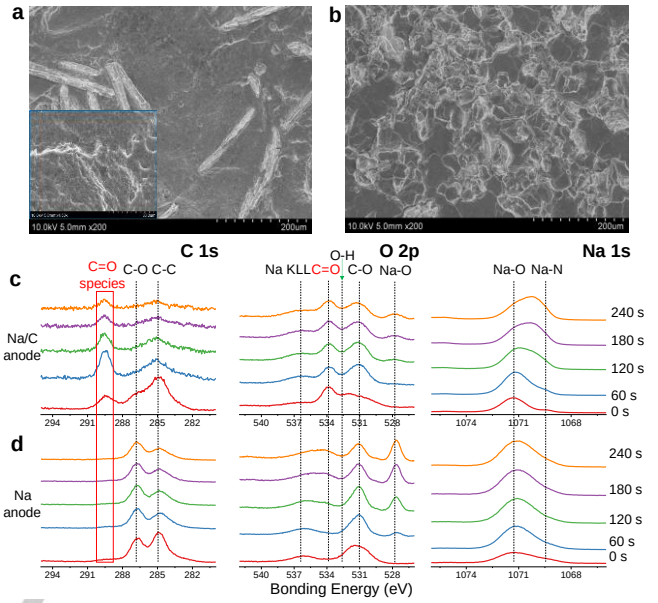

Figure 5. Interface properties after 100 cycles in full cells. SEM images of the Na anodes from (a) Na/C||PEO_{20}NaFSI||$Na_3V_2(PO_4)_3$ cell and (b) Na||PEO_{20}NaFSI|| $Na_3V_2(PO_4)_3$ cell after 100 cycles. XPS C 1s, O 2p and Na 1s spectra for (c) composite Na/C anode and (d) Na-metal anode from full cells.

Next the interface properties were investigated after 100 cycles, the results of which are shown in Figure 5. The composite Na/C electrode displays a relatively flat surface, with exposed carbon fibres sticking out randomly as demonstrated by Figure 5 (a). The enlarged image (Figure S22) shows the rougher morphology of the carbon fibres after cycling than that of the smoother fibres in the pristine carbon cloth. By comparison, the pure Na-metal-foil anode exhibits a fractured and irregular morphology in Figure 5(b). XPS analysis of the surface species at various depths, shown in Figure 5(c) and (d), brings forward the species in both C 1s and O 2p spectra that can be responsible for the chemical bonding between the carbon fibres of the composite Na/C anode and the PEO of the SPE. For the pure Na-metal anode, a large amount of Na-O (mainly representing Na_2O[14]) species are formed at the surface upon cycling. This Na_2O rich interface will unavoidably increase the interface impedance and lead to contact loss because of Na-metal stripping, both promoting to the uneven Na^+ deposition that leads to the downward spiral of interface

degradation. By comparison, the Na/C anode shows a lower amount of Na-O (Na_2O), which enables a better interface contact.

Conclusion

In summary, we have systematically investigated the properties of interface between pure Na-metal anodes and a solid PEO polymer electrolyte. The results suggest that the nature of the interphase, dominated by unavoidable contact loss in combination, which is responsible for early failure of solid-state polymer batteries. A rational strategy to overcome both issues is provided by using a composite Na/C metal anode to replace the Na-metal-foil anode to create a stronger interface connectivity, thereby preventing delamination with the formation of new interface species. The improved interface contact results in a more homogeneous and less fractured Na-plating after repeated cycling, as well as maintaining a low interface impedance. Another factor that is expected to contribute to the more homogeneous plating and stripping is that the high surface area of the carbon fibre, distributing the oxidation/reduction activity *via* the contact points with SPE. During plating this will reduce dendrite formation, and during stripping this will suppress delamination from SPE. The improved interface properties, are reflected in the cycling stability of both symmetric and full Na-metal cells, demonstrating a strongly improved cycling behaviour. All results suggest a promising route towards realizing stable solid-state polymer Na-metal batteries.

Acknowledgements

The research leading to these results has received funding from the National Key Technologies R&D Program, China (2016YFB0901500), the National Natural Science Foundation of China (51725206, 51421002, 51872157), the Strategic Priority Research Program of the Chinese Academy of Sciences (XDA21070500), Beijing Municipal Science and Technology Commission Z181100004718008), Beijing Natural Science Fund-Haidian Original Innovation Joint Fund (L182056) and the Netherlands Organization for Scientific Research (NWO) under the VICI grant nr. 16122. C. Zhao also thanks to the State Scholarship Fund of China Scholarship Council (CSC).

Keywords: Interfacial layer • Solid polymer electrolyte • Composite metal anode • Stable cycling • Sodium batteries

[1] a) V. Palomares, P. Serras, I. Villaluenga, K. B. Hueso, J. Carretero-González, T. Rojo, *Energy Environ. Sci.* **2012**, *5*, 5884-5901; b) H. Kim, H. Kim, Z. Ding, M. H. Lee, K. Lim, G. Yoon, K. Kang, *Adv. Energy Mater.* **2016**, *6*, 1600943; c) P. K. Nayak, L. Yang, W. Brehm, P. Adelhelm, *Angew. Chem. Int. Ed.* **2018**, *57*, 102-120; d) Y. Li, Y. Lu, C. Zhao, Y.-S. Hu, M.-M. Titirici, H. Li, X. Huang, L. Chen, *Energy Storage Mater.* **2017**, *7*, 130-151.e) C. Zhao, M. Avdeev, L. Chen, Y.-S. Hu, *Angew. Chem. Int. Ed.* **2018**, *57*, 7056-7060.
[2] a) H. Yadegari, X. Sun, *Accounts Chem. Res.* **2018**, *51*, 1532-1540; b) C. Zhao, Y. Lu, J. Yue, D. Pan, Y. Qi, Y.-S. Hu, L. Chen, *J. Energy Chem.* **2018**, *27*, 1584-1596; c) Q. Wang, C. Zhao, Y. Lu, Y. Li, Y. Zheng, Y. Qi, X. Rong, L. Jiang, X. Qi, Y. Shao, D. Pan, B. Li, Y.-S. Hu, L. Chen, *Small* **2017**, *13*, 1701835.
[3] Y. Zhao, K. R. Adair, X. Sun, *Energy Environ. Sci.* **2018**, *11*, 2673-2695.
[4] a) C. Zhao, L. Liu, X. Qi, Y. Lu, F. Wu, J. Zhao, Y. Yu, Y.-S. Hu, L. Chen, *Adv. Energy Mater.* **2018**, *8*, 1703012; b) J.-J. Kim, K. Yoon, I. Park, K. Kang, *Small Methods* **2017**, *1*, 1700219.
[5] a) Q. Ma, J. Liu, X. Qi, X. Rong, Y. Shao, W. Feng, J. Nie, Y.-S. Hu, H. Li, X. Huang, L. Chen, Z. Zhou, *J. Mater. Chem. A* **2017**, *5*, 7738-7743; b) J. Serra Moreno, M. Armand, M. B. Berman, S. G. Greenbaum, B. Scrosati, S. Panero, *J. Power Sources* **2014**, *248*, 695-702; c) X. Qi, Q. Ma, L. Liu, Y.-S. Hu, H. Li, Z. Zhou, X. Huang, L. Chen, *ChemElectroChem* **2016**, *3*, 1741-1745; d) A. Chandra, A. Chandra, K. Thakur, *Eur. Phys. J. Appl. Phys.* **2015**, *69*.
[6] a) X. Yu, L. Xue, J. B. Goodenough, A. Manthiram, *ACS Mater. Lett.* **2019**, 132-138; b) W. Zhou, Y. Li, S. Xin, J. B. Goodenough, *ACS Cent. Sci.* **2017**, *3*, 52-57; c) X.-X. Zeng, Y.-X. Yin, N.-W. Li, W.-C. Du, Y.-G. Guo, L.-J. Wan, *J. Amer. Chem. Soc.* **2016**, *138*, 15825-15828; d) W. Zhou, S. Wang, Y. Li, S. Xin, A. Manthiram, J. B. Goodenough, *J. Amer. Chem. Soc.* **2016**, *138*, 9385-9388; e) P. R. Chinnam, S. L. Wunder, *ACS Energy Lett.***2017**, *2*, 134-138.
[7] S. Song, Z. Dong, C. Fernandez, Z. Wen, N. Hu, L. Lu, *Mater. Lett.* **2019**, *236*, 13-15.
[8] a) Y. Liu, D. Lin, Y. Jin, K. Liu, X. Tao, Q. Zhang, X. Zhang, Y. Cui, *Sci. Adv.* **2017**, *3*, eaao0713; b) J. Wan, J. Xie, X. Kong, Z. Liu, K. Liu, F. Shi, A. Pei, H. Chen, W. Chen, J. Chen, X. Zhang, L. Zong, J. Wang, L.-Q. Chen, J. Qin, Y. Cui, *Nature Nanotech.* **2019**, *14*, 705–711.
[9] S. Lv, T. Verhallen, A. Vasileiadis, F. Ooms, Y. Xu, Z. Li, Z. Li, M. Wagemaker, *Nat. Commun.* **2018**, *9*, 2152.
[10] L. Pauling, *The Nature of the Chemical Bond, 3rd Edition, Cornell University Press, Ithaca,* **1960**.
[11] a) Y. Zhao, X. Yang, L.-Y. Kuo, P. Kaghazchi, Q. Sun, J. Liang, B. Wang, A. Lushington, R. Li, H. Zhang, X. Sun, *Small* **2018**, *14*, 1703717; b) W. Luo, Y. Zhang, S. Xu, J. Dai, E. Hitz, Y. Li, C. Yang, C. Chen, B. Liu, L. Hu, *Nano Lett.* **2017**, *17*, 3792-3797; c) A. Wang, X. Hu, H. Tang, C. Zhang, S. Liu, Y.-W. Yang, Q.-H. Yang, J. Luo, *Angew. Chem. Int. Ed.* **2017**, *56*, 11921-11926.
[12] a) S.-S. Chi, X.-G. Qi, Y.-S. Hu, L.-Z. Fan, *Adv. Energy Mater.* **2018**, *8*, 1702764; b) D. Lin, Y. Liu, Z. Liang, H.-W. Lee, J. Sun, H. Wang, K. Yan, J. Xie, Y. Cui, *Nature Nanotech.* **2016**, *11*, 626; c) C. Yang, Y. Yao, S. He, H. Xie, E. Hitz, L. Hu, *Adv. Mater.* **2017**, *29*, 1702714.
[13] a) K. Li, J. Zhang, D. Lin, D.-W. Wang, B. Li, W. Lv, S. Sun, Y.-B. He, F. Kang, Q.-H. Yang, L. Zhou, T.-Y. Zhang, *Nat. Commun.* **2019**, *10*, 725; b) J. Zhang, D.-W. Wang, W. Lv, S. Zhang, Q. Liang, D. Zheng, F. Kang, Q.-H. Yang, *Energy Environ. Sci.* **2017**, *10*, 370-376.
[14] a) J. Zheng, S. Chen, W. Zhao, J. Song, M. H. Engelhard, J.-G. Zhang, *ACS Energy Lett.***2018**, *3*, 315-321; b) B. Zhang, G. Rousse, D. Foix, R. Dugas, D. A. D. Corte, J.-M. Tarascon, *Adv. Mater.* **2016**, *28*, 9824-9830.

Entry for the Table of Contents

RESEARCH ARTICLE

Through preparation of a composite Na/C metal anode, an effective approach is introduced that *in-situ* constructs a strong chemical connection between the composite anode and the PEO based polymer electrolyte. This interconnected interface environment results in ultralong cycle life of Na-metal polymer batteries, reaching a capacity retention of >80% after 5,000 cycles.

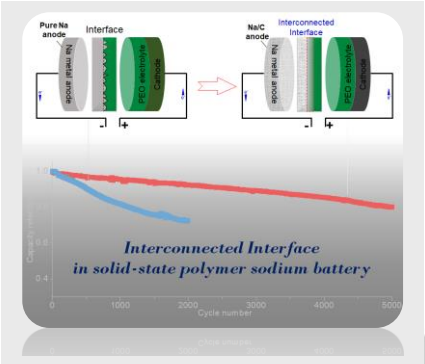

Chenglong Zhao, Lilu Liu, Yaxiang Lu, Marnix Wagemaker*, Liquan Chen, and Yong-Sheng Hu**

Page No. – Page No.

Revealing an Interconnected Interfacial Layer in Solid-State Polymer Sodium Batteries